



## Industrial application of ceramic nanofiltration membranes for water treatment in oil sands mines

Sandra Motta Cabrera<sup>a</sup>, Louis Winnubst<sup>a,\*</sup>, Hannes Richter<sup>b</sup>, Ingolf Voigt<sup>b</sup>, Arian Nijmeijer<sup>a</sup>

<sup>a</sup> *Inorganic Membranes, MESA + Institute for Nanotechnology, University of Twente, P.O. Box 217, 7500 AE Enschede, the Netherlands*

<sup>b</sup> *Fraunhofer Institute for Ceramic Technologies and Systems, Michael-Faraday-Str. 1, 07629 Hermsdorf, Germany*

### ARTICLE INFO

#### Keywords:

Ceramic membranes  
Nanofiltration  
Oil sands mines  
Recycle process water  
Water treatment

### ABSTRACT

A commercial titania ceramic nanofiltration membrane unit with a permeate flow capacity of 20 m<sup>3</sup>/h was used to reduce ion concentration, Total Suspended Solids (TSS) and Total Organic Carbon (TOC) in recycle water from a Canadian oil sands mine. This unit, the first of its kind, was tested for almost two years to evaluate membrane performance under actual recycle process water conditions. This paper focuses on the results at a 50% stage cut. A strong correlation between specific flux and rejection was found, with the highest mass rejections observed at the lowest specific flux values. A potential formation of a cake layer on the membrane surface seems to favour the rejection since lower specific flux values improved mass rejection. The analysis of more than 20 ions showed that differences in hydrated ionic sizes and electrostatic phenomena are at play with divalent cations showing the largest rejection. Additional 75–90% TOC and almost 100% TSS rejection was observed. These results indicate that it is possible to implement this technology in an oil sands mine and obtain significant water quality improvements and reducing river water intake.

### 1. Introduction

Mineable oil sands constitute an important source of crude oil to the worldwide market, with production accounting for approximately 1.5 million barrels per day, almost entirely coming from Canadian oil sands deposits [1]. These oil sands are unconsolidated sand deposits consisting of solids (silica sand, quartz, silts, and fine clays ca. 85 wt%), water (3–6 wt%), and bitumen (0–16 wt%), which is a high molar mass viscous petroleum fluid. Canada and Venezuela have the two largest sources of bitumen in the world, with resources comparable to those of the conventional oil deposits worldwide. In Canada, over 95% of the known in-place oil volumes are in three areas in Northern Alberta: Athabasca, Peace River, and Cold Lake [2]. The Athabasca deposit, the largest Canadian oil sands deposit, is the only resource shallow enough to be partially amenable to open-pit mining techniques [3].

Once the oil sands are mined, the bitumen is separated from the sand through contact with hot water. The extraction process mainly operates at a ratio of 9 barrels of water per barrel of oil [4]. Consequently, water is a key natural resource to the production of the oil sands. The water sources for the extraction process are typically nonsaline water (i.e. surface river, runoff water, and nonsaline groundwater) [5] from nearby

sources (5–20%) and existing recycled process water (80–95%) [6]. Furthermore, water is a very important oil sands process parameter because once river water enters the mines sites and becomes produced or recycle process water, it cannot be discharged back to the environment as per governmental “zero discharge policy” [7]. This policy ensures that the quality of the river water is maintained, and the health of aquatic creatures is protected [8]. This situation creates two major challenges for the oil sands industry: (a) maintaining dissolved ions and solids of recycle process water at adequate concentrations to avoid any detrimental effects on oil recovery and process equipment; (b) creation of large tailings ponds as containment facilities for the recycle process water. The tailings stream from the process is a slurry composed of approximately 44 wt% water, 1 wt% residual bitumen, and 55 wt% solids, of which 82 wt% is sand, and 17 wt% are solids smaller than 44 μm (fines solids). Salts, surfactants, naphtha, hexane and other light hydrocarbons may also be present in the tailings mixture [9]. When tailings streams are discharged into the tailings ponds, the coarse solids settle out rapidly in areas nearby the edge (beach) whereas residual bitumen, fines and water are carried in the run-off slurry. Some of the fines start settling across the tailings pond, but it takes several years to reach complete settling without any chemical addition. During the tailings deposition in the ponds, a “free water” zone containing few

\* Corresponding author.

E-mail address: [a.j.a.winnubst@utwente.nl](mailto:a.j.a.winnubst@utwente.nl) (L. Winnubst).

<https://doi.org/10.1016/j.seppur.2020.117821>

Received 20 May 2020; Received in revised form 23 September 2020; Accepted 28 September 2020

Available online 6 October 2020

1383-5866/© 2020 The Author(s). Published by Elsevier B.V. This is an open access article under the CC BY license (<http://creativecommons.org/licenses/by/4.0/>).

### Nomenclature

Symbol	Description [Units]
CIP	Cleaning in Place [-]
CFS	Coagulation-flocculation-sedimentation [-]
Da	Dalton [-]
IC	Ion chromatography [-]
ICP	Inductively coupled plasma [-]
IEP	Isoelectric point [-]
Re	Reynolds number [-]
SAGD	Steam assisted gravity drainage [-]
TMP	Transmembrane pressure [bar]
TNU	Titania Nanofiltration Unit [-]
TOC	Total Organic Carbon [mg/kg]
TDS	Total Dissolved Solids [mg/kg]
TSS	Total Suspended Solids [mg/kg]

solids is formed, as shown in Fig. 1. This free water, containing organic components such as naphthenic acids and sulphonates, is pumped out and recycled as process water in the extraction process. Furthermore, this recycle process water contains many electrolyte species, such as  $\text{Cl}^-$ ,  $\text{SO}_4^{2-}$ ,  $\text{HCO}_3^-$ ,  $\text{Ca}^{2+}$ ,  $\text{Mg}^{2+}$ , and  $\text{Na}^+$  [10], which can cause fouling and scaling in downstream systems.

Fig. 2 shows a scheme of a typical water system in an oil sands mine. Two water sources are used in the oil sands process: river water and recycle process water. The river water that enters the mine site is stored in a river water pond to be subsequently distributed either to utilities area for steam production in boilers or as a gland water for a pumping system located at the extraction plant. In this plant, separation of oil from water and sand occurs and tailings are generated as a by-product. These tailings are subsequently pumped to the tailings ponds where “free water” is produced. This water is collected in a “recycle process water” pond that supplies almost all the water demand required by the oil extraction plant. Due to the importance of this recycle process water pond, daily water quality controls are performed to ensure concentrations of ions, suspended solids, and organic material are under established operational limits.

The large water consumption required in the oil sands industry has highlighted the need for looking into different alternatives to reduce river water intake or increase the use of existing recycle process water. This need is currently one of the key drivers of the sustainability programs of these mines. Typical water treatment technologies in oil sands mines include a combination of clarifiers, microfiltration membranes, softeners, and reverse osmosis. A promising alternative for the previous described water treatment within the oil sands industry is the use of ceramic nanofiltration membranes due to their excellent chemical resistance to inorganic acids and oxidants, the tolerance to high temperatures and longer life span than polymeric membranes [10]. Several studies have been conducted to treat oil-containing wastewater using ceramic membranes. These studies showed that ceramic membranes

perform better than polymeric membranes on oil-containing waters [11,12]. Furthermore, ceramic membranes with a pore size in the (sub) nanometer range can reject significant amounts of solids, bitumen and electrolytes that are present in the recycle process water due to the size of these components.

Very few studies about the use of nanofiltration membranes to treat oil sands process water are available in the open literature, and most of these studies use polymeric membranes. Peng et al. [13] studied the performance of three different commercial polymeric flat sheet nanofiltration membranes in well-controlled, bench-scale experiments. The membranes were used to treat different types of oil sands process water (imported and potential discharge waters from a mine site). Performance was focused on removal of polyvalent ions (reduction of hardness) and naphthenic acids due to its toxicity. The use of these membranes showed a significant reduction in water hardness and naphthenic acids (>95%). Even though the membranes fouled during the tests, it was found that the fouling was reversible. Kim et al. [14] investigated the application of nanofiltration and reverse osmosis membranes to remove salt ions in the oil sands process water and studied the effect of pre-treatment methods such as coagulation-flocculation-sedimentation (CFS) with and without the use of coagulants and coagulant aids. Experiments were performed using a lab-scale membrane cross-flow filtration module and two nanofiltration polymeric flat-sheets membranes. Results show that addition of coagulants to the pre-treatment CFS process provided higher elimination of salts than only gravity settling, and this helps to reduce membrane fouling and improved membrane performance (~69% and 82% NaCl removal with and without pre-treatment respectively) [14]. Sadrzadeh et al. [15] studied the use of polymeric nanofiltration membranes in different water treatment processes of an in-situ heavy oil recovery method called SAGD (steam assisted gravity drainage). This process, which is widely used for bitumen extraction from oil sands in Canada, uses produced water to generate steam, which is injected through a horizontal well into the bitumen-containing formation to decrease the viscosity of the bitumen and allow its extraction. This produced water, in comparison to recycled process water from an oil sands mine as discussed in this work, has in general higher pH values (9–10.5 vs. 7.3–9.0), higher TOC (420–500 vs. 46–85 mg/L) and lower calcium and magnesium concentration (0.84–2.5 vs. 30–80 mg/L). These SAGD produced water ranges are representative of boiler feed water and warm lime softeners. The membranes used by Sadrzadeh et al. were thin film composites consisting of three layers: a thin polyamide or sulfonated polyethersulfone active layer (100–300 nm), an intermediate microporous layer (~40  $\mu\text{m}$ ), and a mesoporous polyester non-woven fabric support (~100  $\mu\text{m}$ ). Results shows a removal of up to 98% of the total dissolved solids (TDS), total organic carbon (TOC), and dissolved silica, and more than 99% removal of divalent ions was achieved using commercial polymeric nanofiltration membranes.

For mining industry applications, no testing of ceramic nanofiltration membranes has been done at commercial scale. Loganathan et al. [16] used a pilot-scale membrane system in an oil sands mine to study the effects of different pre-treatment technologies on the performance of ceramic ultrafiltration membranes during the treatment of oil sands recycle process water. This system consisted of two treatment trains operated in parallel. Treatment train 1 used coagulant addition prior to the ceramic ultrafiltration system, and treatment 2 included softening and coagulant addition, followed by the ceramic membrane system. The treatment trains consisted of titania membrane elements (CeraMem® FE-S2S- 0100TO-D00-00) with a nominal average pore size of 0.1  $\mu\text{m}$ . Results show that coagulant addition was necessary for almost complete solids removal and membrane fouling could be reduced by the addition of a softening step as pre-treatment.

Overall, these studies show that nanofiltration technology could be applied in the water treatment of oil sands with significant reduction (up to 95%) in organic components and electrolytes. However, the studies also show that the use of polymeric membranes require either chemical



Fig. 1. Segregation profile of tailings ponds.

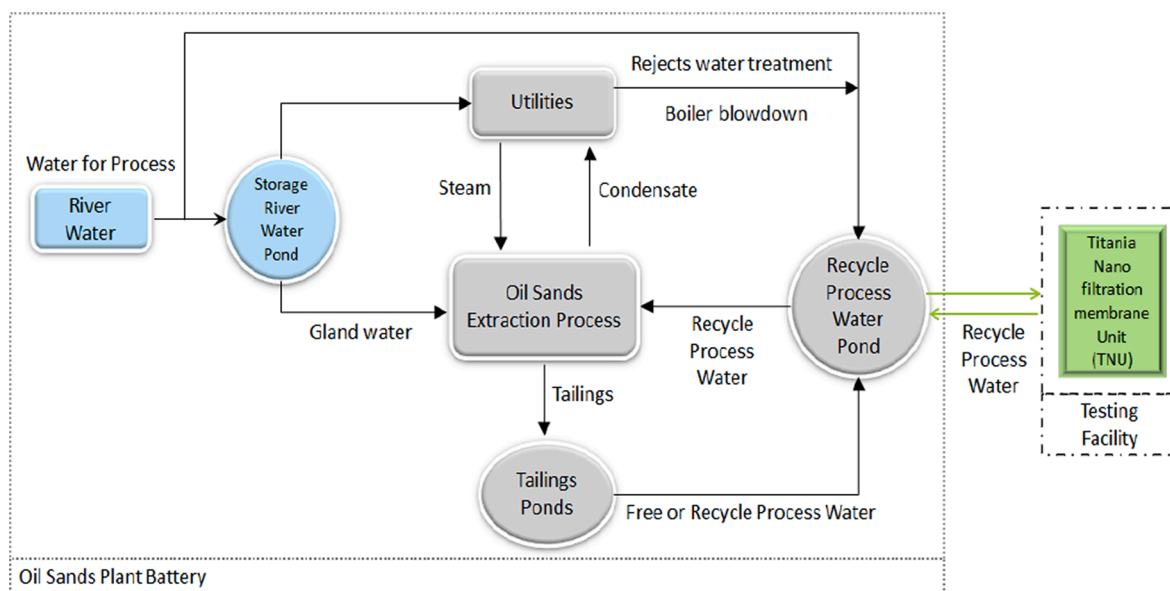


Fig. 2. Overall water system in an oil sands mine and TNU testing facility.

or physical pre-treatment technologies to avoid rapid detrimental effects from organic acid and solids content present in the water streams. Note that ceramic membranes, in comparison to polymeric membranes, show better resistance against mechanical, thermal, and chemical stress [17,18]. They are also easier to maintain, have a longer lifespan, and do not swell or compact [19,20]. In addition, the small pore size of these membranes provides the potential to meet the current water treatment effluent standards with no chemical pre-treatment [21,22].

Based on the potential benefits of using ceramic nanofiltration technology in the oil sands mine industry, the first of its kind commercial pilot unit with titania membranes (Titania Nanofiltration membrane Unit - TNU) was built and installed in a Canadian oil sands mine to determine its performance in a 24/7 production operation. This technology could be used as a pre-treatment stage upstream of the reverse osmosis unit. Alternatively, the water produced from these ceramic membranes could be fed directly to boilers if this water has the required quality characteristics to produce steam. Another potential application in the Oil Sands Extraction Process is the treatment of warm water coming from thickener overflow. This means that instead of sending this water stream to the tailings ponds, where it will be cooled down to ambient temperature, the stream would be reused in the extraction process. Thereby, saving on heating costs and reducing greenhouse gas emissions.

The economic feasibility of implementing ceramic nanofiltration membranes in the oil sands industry would depend on the desired application and potential operating savings in the long term (e.g. feed to the existing conventional reverse osmosis system in an oil sands mine for further polishing vs. treatment of warm thickener overflow water). The potential savings could be quantified in terms of amount of fresh water withdrawn from the river, as well as energy savings and reduction of greenhouse gases emissions. As a reference, a Mine Waste Technology program 2002 annual report compared the investing and operating costs of polymeric and ceramic membrane systems with a capacity of 1,136 l/min. The capital cost of a ceramic membrane system was approximately 1,900,000 USD vs. 1,800,000 USD for a polymeric membrane system (about 5% difference). The annual operating costs of a ceramic membrane system was about 55% less than the similar capacity polymeric membrane system due to lower maintenance cost of ceramic membranes. In general, the usage of ceramic membranes in treatment of mining effluents show more long-term advantages such as durability, better chemical and mechanical stability, and lower annual operational costs in comparison to polymeric membranes [23].

The Titania Nanofiltration Unit of this study was located next to a recycle process water pond which supplies most of the water to the oil sands extraction process (see Fig. 2). The TNU was fed with the same water quality used in oil sands processing at real-time production conditions (e.g. bitumen content, soluble ions, dispersed solids). This means that any type of operational upsets, present in the recycle process water, such as high solids content or TOC, was immediately observed at the TNU facility. The location of the TNU was temporary and only for the testing; however, this location may be suitable for future commercial implementation.

The work described in this paper focuses on the evaluation of the performance of titania nanofiltration membranes treating actual oil sands recycle process water, without any type of chemical or mechanical pre-treatment. This work also focuses on understanding the most dominant mechanisms that impact the membrane performance. Performance has been measured as water quality (ion rejection, TSS and TOC reduction). To the authors' knowledge, the use of titania nanofiltration membranes in an oil sands mine at a commercial scale, as described in this work, is a novel approach in this industry. This application is the first attempt at understanding the performance of ceramic nanofiltration membranes under actual operation conditions in a 24/7 production operation.

## 2. Equipment and system description

### 2.1. Commercial titania nanofiltration unit (TNU)

The Titania Nanofiltration Unit (TNU) is a fully automated membrane filtration unit, requiring minimal attention from an operator. The unit consists of two 12.2 m sea-containers equipped with internal heaters to avoid freezing of pipelines and equipment during winter conditions because ambient temperatures in the northern of Alberta in Canada can reach values as low as  $-40^{\circ}\text{C}$ . The TNU has four insulated membrane modules in series (Fig. 3).

The TNU process flow diagram is shown in Fig. 4. Recycle process water, without any pre-treatment, is fed to the unit through a slip stream that comes from the main recycle process water pipeline. This slip stream supplies recycle process water to a feed pump in the TNU that brings up system pressure into a recycle loop. An additional recycle pump is used to create crossflow velocity over the membrane to keep the water in a turbulent state to minimize fouling. Clean water is permeated through the membrane and is collected in a permeate tank. At set times a



Fig. 3. Titania Nanofiltration Unit (TNU).

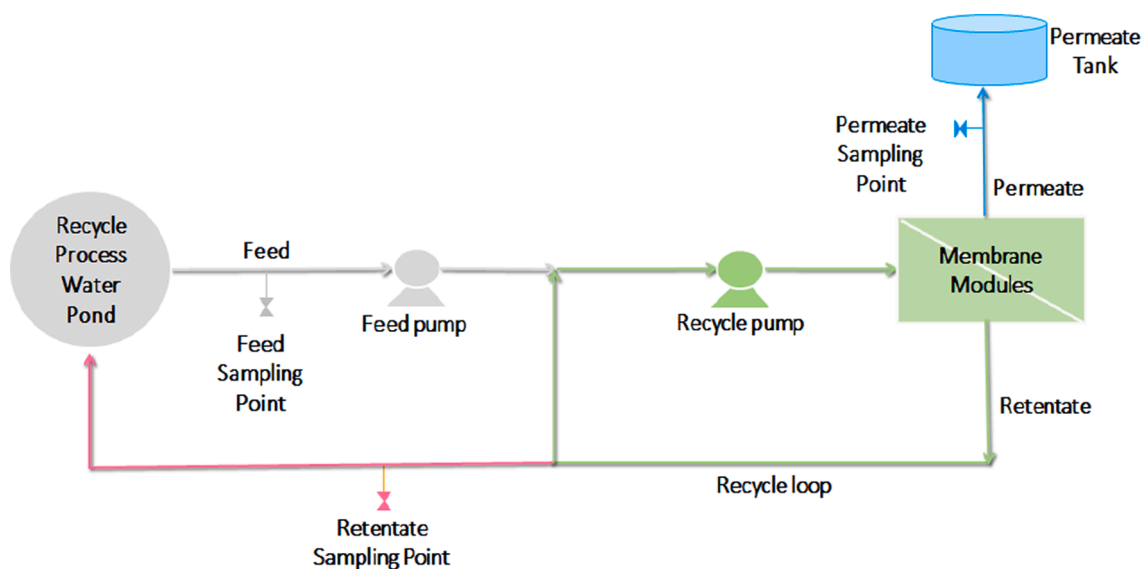


Fig. 4. TNU process flow diagram.

backflush is automatically initiated to clean the membranes by flushing back a limited amount of permeate water through the membrane. The retentate (or concentrate), is extracted from the recycle loop via a backpressure controller and sent back to the recycle process water pond. The discharge location of the retentate is different from where the recycle feed water to the TNU is initially supplied to avoid cross-contamination. Each of the streams in the unit is equipped with a sampling point, flowmeters and pressure gauges. The TNU also contains an automatic cleaning in place (CIP) system that is activated if the membrane has been fouled to such an extent that backflush cannot clean the membrane effectively. In a CIP cycle, the membrane is automatically cleaned with caustic soda (NaOH) and citric acid solutions to render the membrane back to its initial performance. Caustic soda helps to remove organic foulants and citric acid is used to remove scales and metal oxides [24]. The caustic soda and citric acid solutions are stored in two tanks embedded within the TNU facility. The system has two pressure relief valves, which open when reaching the design pressure to avoid further pressure increase. A series of analog and digital sensors are installed in the TNU to monitor any potential high or low value alarms for safety and to ensure the integrity of the system. If an alarm occurs, the unit switches off and closes all valves to prevent fluid release. The alarms in the system are triggered by low and high temperature and pressure in the membrane loop, low volumetric flow in membrane loop, low and high volumetric flow in the permeate line, low and high levels in the CIP tanks, and high temperature in the CIP tanks.

The unit also has a small lab area where samples of feed, permeate, and retentate are taken by an operator. The entire TNU system is

operated using a touch panel which is installed in a control cabinet. Measured values such as temperature, pressures and volumetric flows are recorded in the unit every 30 min. Table S1 (Supporting Information) shows the main design specifications and available ranges that can be introduced as settings in the TNU system.

## 2.2. Ceramic membranes

Each membrane module or housing in the TNU contains 45 titania membranes (Fig. 5a). Each membrane, with a length of 1,200 mm has 151 channels (Fig. 5b) with an approximate diameter of 2 mm. The total surface area per module is 58.5 m<sup>2</sup>. The titania membranes used in the unit are cylindrical, multi-layered with a final separation layer having nano-sized pores (0.9 nm in average) determined by N<sub>2</sub> sorption [25]. The main properties of the membrane according to supplier, Inopor, are shown in Table 1.

Fig. 6 displays a SEM image of the membrane. The mean thickness of the first titania layer (from left to right in the figure) is 0.5 μm with a pore size of 5 nm. The zirconia intermediate layer with a pore size of 3 nm and the final titania/zirconia separation layer with a pore size of 0.9 nm cannot be individually distinguished in Fig. 6. The total thickness of both layers was 100 nm. The separation layer was applied on the support through a polymeric sol-gel technique based on a titanium isopropoxide precursor [26].

The metal oxides in the separation layer (titania and zirconia) show amphoteric behaviour in water, meaning that they can act as acids or bases (donating or receiving protons) depending on the pH of the

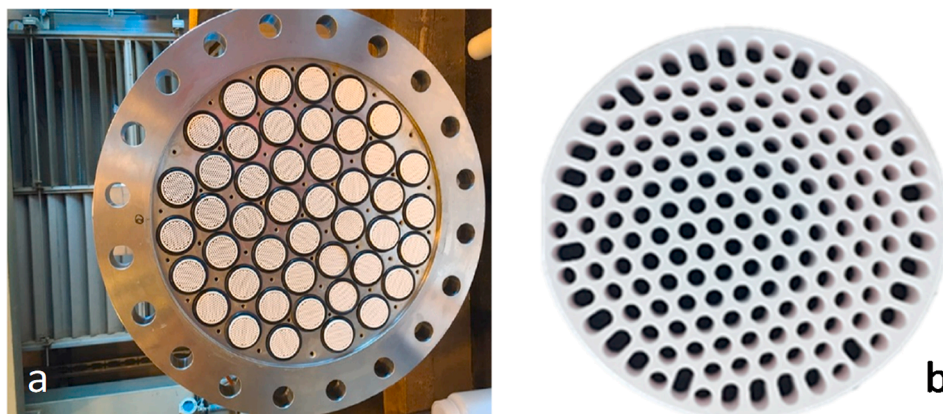
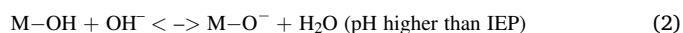


Fig. 5. a) TNU Module with 45 membranes. b) Close up of an individual membrane element showing 151 channel [26].

**Table 1**  
Titania (TiO<sub>2</sub>) Membrane Properties.

TiO <sub>2</sub> Membrane Properties	Value	Reference
Mean pore size	0.9 nm	[26]
Membrane surface area	1.3 m <sup>2</sup> /element	[26]
Pure water flux range (at 1 bar)	15–20 l/m <sup>2</sup> ·h	[26]
Cut off molecular weight	450 Da	[27]
Maximum temperature	400 °C	[27]
Pressure stability	≥ 60 bar	[27]

solution. These oxides also carry no net electrical charge at a pH known as the isoelectric point (IEP). Knowledge of pH of the solvent stream is a key parameter when using ceramic membranes because it determines the membrane surface charge based on its IEP. pH values below the IEP lead to a positive charge on the ceramic membrane, and pH values above the IEP initiate a negative charge [28]. The predominant functional groups of the membrane depending on pH are M–OH<sub>2</sub><sup>+</sup> and M–O<sup>–</sup>, where M is the titanium/zirconium metal, as per following reactions [29]:



The hydroxyl groups on the left side of these reactions are formed from the metal oxides by dissociative chemisorption of water molecules, and it is generally considered that hydration happens at exposed lattice metal ion site on the surface of the metal oxides since the lattice metal ions are strong Lewis acids [30].

Fig. 7 shows the surface of the nanofiltration membrane. After inspection, it was concluded that most of the surface of the membrane is defect-free. Small imperfections like bumps and buckles were covered during manufacturing (Fig. 7a). Only at the outer walls of the outer channels, some defects were detected (Fig. 7b) [26].

### 3. Experimental design

#### 3.1. Operational program

A TNU experimental philosophy was designed to evaluate the ion rejection and most dominant mechanisms involved when using titania membranes to treat oil sands process recycled water. The TNU was tested for almost two years in a 24/7 oil sands mine operation. Table 2 shows the main TNU independent parameters, inputs and outputs during the testing program at 50% stage cut.

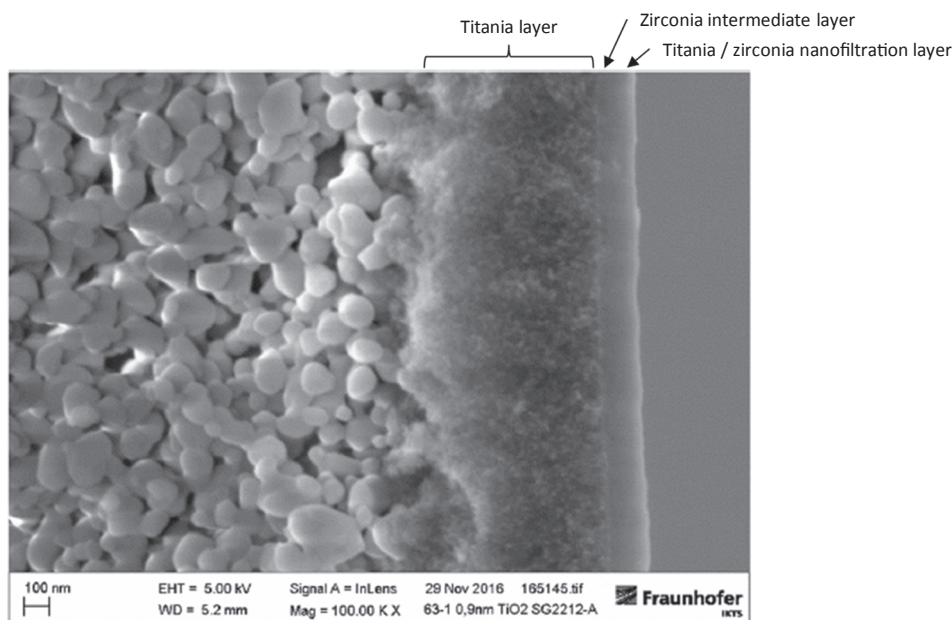


Fig. 6. Membrane SEM image [26].

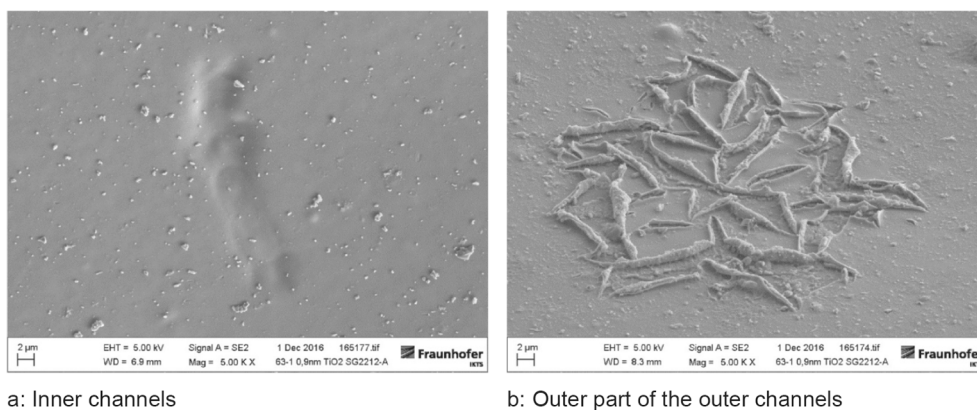


Fig. 7. Surface of the Nanofiltration Membrane [26].

Recycle process water feed properties such as temperature, pH, ions and solids concentration were considered independent variables because they changed in a daily basis as result of a real-time oil sands extraction process, and consequently, no control could be exerted over these variables. The TNU system was operated during winter, spring, summer, and fall.

In terms of control variables, the TNU can be tested in either constant stage cut (permeate yield) or constant transmembrane pressure (TMP) mode. The use of constant stage cut mode means that a predetermined stage cut value is introduced as a set point into the system. The system, in turn, will use trans membrane pressure to maintain the stage cut set point, by eventually rising the TMP as the operation continues. The typical ranges for the other control variables shown in Table 2 were a cross-flow velocity of 2 m/s, and backflush frequency and duration of 15 min and 15 sec, respectively. These values were determined after preliminary testing of the unit during commissioning and were introduced as pre-set values on the settings function of the unit. The chemical cleaning frequency was performed either automatically or manually when the specific flux reached low pre-set values, which depended mostly on the feed water TSS and solids content. Specific Flux, a measure of the flux of a fluid through a membrane, was calculated as the ratio between flux and TMP.

The volumetric flows of feed, permeate, and retentate streams were measured using electromagnetic flow sensors. The temperature of the recycle process to the unit was also measured through a thermocouple located on the feed stream. Tracking of pre-set values such as stage cut, cross-flow velocity, backwash frequency, duration and pressure was also performed during the entire TNU operation. The flow regime in the membrane elements was checked by calculating Reynolds number (Re) as shown in Eq. (1) [24], where  $\nu$  is the relative velocity of the recycle feed water in the filtration loop,  $\phi$  is the hydraulic diameter of one

membrane channel,  $\rho$  is recycle feed water density that was calculated using the weight fractions of bitumen, water and solids present in the feed, and the recycle feed water viscosity was calculated using water viscosity ( $\mu_w$ ) and Einstein equation for fluids with <0.02 vol fraction ( $\Theta$ ) of solids particles [31].

$$Re = \frac{\nu\phi\rho}{\mu_w(1 + 2.5\Theta)} \tag{3}$$

The TMP in crossflow filtration is an average between the pressure on permeate and retentate sides. The flux was calculated by the system as the ratio between permeate volumetric flow and membrane surface area per module (58.5 m<sup>2</sup>).

### 3.2. Recycle water analytical sampling program

TNU samples of the feed, permeate, and retentate streams were taken either weekly or biweekly depending on operational resources. The collection of samples was done manually using purge valves located in the streams. The sampling program included Dean-Stark and water chemistry analyses in all three streams. Dean-Stark analysis (a distillation assay) was used to determine solids, water and bitumen content [32]. The solids content was also used to calculate the density of each stream and consequently convert volumetric flows to mass flows. Water chemistry analysis included determination of pH, major cations, anions, as well as other components such as total organic carbon (TOC), total suspended solids (TSS), total dissolved solids (TDS), hardness, and silica. Testing was performed in a third-party lab. Cations and anions were analyzed using ICP (inductively coupled plasma) and ion chromatography (IC) respectively. Bicarbonate (HCO<sub>3</sub><sup>-</sup>) was measured by titration. TSS was detected using a standard method for the examination of water and wastewater that uses a suction filtration apparatus and drying the solids at 103–105 °C, TDS was measured as the material passing through a Whatman 934-AH filter paper and remaining in a crucible after evaporation and drying at 180 °C, while TOC was measured through a high temperature combustion method [33]. Table 3 includes a list of 22 ions and compounds analyzed during the TNU sampling program. These ions and components are analyzed on the recycle process water of this oil sands mine to determine potential impact on oil recovery.

The results obtained from this analytical sampling program were used to analyze the performance of the membranes in terms of ion or component mass rejection (Eq. (4)).

$$\text{Mass rejection} = 1 - \frac{\dot{m}_{\text{permeate}} * [\text{ion}]_{\text{permeate}}}{\dot{m}_{\text{feed}} * [\text{ion}]_{\text{feed}}} \tag{4}$$

Here,  $\dot{m}_{\text{permeate}}$  and  $\dot{m}_{\text{feed}}$  are mass flow of permeate and feed respectively, and [ion] represents ion or component concentration in either permeate or feed. The mass flows of feed and permeate are calculated by multiplying the volumetric flow of each stream by its density. The

Table 2  
TNU Parameters: Experimental Design.

Independent Parameters	Inputs	Outputs
Recycle process water feed:	Operational mode; Constant:	<ul style="list-style-type: none"> <li>■ Volumetric flows of feed</li> <li>■ permeate, and retentate streams</li> <li>■ Transmembrane pressure (TMP)</li> <li>■ Flux</li> <li>■ Specific Flux</li> <li>■ Water Quality</li> <li>■ Chemical cleaning frequency</li> </ul>
<ul style="list-style-type: none"> <li>■ Temperature</li> <li>■ pH</li> <li>■ Ions concentration</li> <li>■ Solids concentration</li> </ul>	<ul style="list-style-type: none"> <li>■ Stage cut (permeate yield)</li> <li>■ Cross flow velocity</li> <li>■ Backwash frequency</li> <li>■ Backwash duration</li> </ul>	

**Table 3**  
TNU Lab Analysis.

Cations	Anions	Compounds
<ul style="list-style-type: none"> <li>■ Sodium, Na<sup>+</sup></li> <li>■ Potassium, K<sup>+</sup></li> <li>■ Lithium, Li<sup>+</sup></li> <li>■ Calcium, Ca<sup>2+</sup></li> <li>■ Magnesium, Mg<sup>2+</sup></li> <li>■ Barium, Ba<sup>2+</sup></li> <li>■ Manganese, Mn<sup>2+</sup></li> <li>■ Copper, Cu<sup>2+</sup></li> <li>■ Iron, Fe<sup>2+,3+</sup></li> <li>■ Aluminum, Al<sup>3+</sup></li> <li>■ Phosphorus, P<sup>3+</sup></li> </ul>	<ul style="list-style-type: none"> <li>■ Chlorine, Cl<sup>-</sup></li> <li>■ Fluorine, F<sup>-</sup></li> <li>■ Bromine, Br<sup>-</sup></li> <li>■ Bicarbonate, HCO<sub>3</sub><sup>-</sup></li> <li>■ Sulphate, SO<sub>4</sub><sup>2-</sup></li> <li>■ Nitrite, NO<sub>2</sub><sup>-</sup></li> <li>■ Nitrate, NO<sub>3</sub><sup>-</sup></li> <li>■ Phosphate, PO<sub>4</sub><sup>3-</sup></li> </ul>	<ul style="list-style-type: none"> <li>■ Bitumen</li> <li>■ Solids</li> <li>■ TOC</li> <li>■ TSS</li> <li>■ TDS</li> <li>■ Hardness (as CaCO<sub>3</sub>)</li> <li>■ Silica (SiO<sub>2</sub>)</li> <li>■ Total Silicon, Si</li> <li>■ Total Sulphur, S</li> <li>■ Total Boron, B</li> </ul>

density of the streams is a function of the recycle water temperature and the solids content. Although ion rejection is typically used to monitor membrane performance, the authors prefer to use mass rejection to capture the different fluctuations in recycle water (e.g. temperature, density and volumetric flow) resulting from testing the ceramic membrane unit in a real 24/7 oil sands mine operation. By using mass rejection, the noise generated by these fluctuations is diminished.

#### 4. Results and discussion

The TNU was operated throughout the year; therefore, the temperature of the recycle process water, feed to the unit, ranged between 6 and 36 °C. pH values varied between 7.7 and 8.4 as part of normal daily operations; hence, the recycle process water is generally a mild basic solution. As previously mentioned in Section 2.2, pH values below the isoelectric point (IEP) of the ceramic membrane lead to have a positive charge, and pH values above the IEP initiate a negative charge. As the IEP of titania/zirconia is between 5.3 and 6.9 [34], it can be assumed that the membranes in the TNU system had a negative surface charge during the testing. Although absorbed organic matter may change the IEP of the membrane surface, it is considered that the number of ions present in the recycle process water might be larger than the organic matter, which means that the ions might have a stronger electrical charge effect over the membrane.

While the TNU was operating at a 50% stage cut for approximately 75 days (around 1,800 h), the system was fed with an average recycle process water flow of 7.0 m<sup>3</sup>/h and a maximum of 9.5 m<sup>3</sup>/h. During this operating mode, the TMP increased gradually over time to maintain the stage cut at constant set point. The highest TMP value reached was 13.3 bar for this dataset. A specific flux reduction over time was observed, indicating that some fouling occurred. In this context, fouling is defined as the process resulting in loss of specific flux due to the deposition of suspended or dissolved substances on the external surface of the membrane, in its pore openings, or within its pores [24]. The sub nanometer size (0.9 nm) of the pores in the TNU was designed to prevent as much as possible intrusion of particulates in the ceramic support. Therefore irreversible fouling, resulting from strong chemical or physical sorption of particles and solutes in the pores, is mitigated [22].

As a quality assurance and control measure, the mass flows of feed, permeate, and retentate were back-calculated, using density and measured volumetric flows. The objective was to compare calculated vs. experimental values and to evaluate the accuracy of the data. The differences between actual and calculated mass flows for the three streams were found to be within 10%. These results show very good data consistency of inlet and outlet flows from the TNU system.

The measured concentration ranges in the recycle feed water for

cations, anions, and other components such as solids, TOC, TSS, calcium carbonate, and silica are presented in Table 4. This database was comprised of 28 samples taken in 11 months. The highest content material present in the recycle process water were found to be solids, followed by TSS, calcium carbonate, TOC, and total sulphur. Sodium was the cation with the highest concentration followed by calcium. Bicarbonate, sulfate, and chlorine showed the highest concentrations among the anions, in that order. Copper, iron, manganese, nitrite, aluminum, phosphorus, and phosphate were found in trace quantities.

Overall, the average standard deviation for the concentration of cations and anions in the feed water is 20%. On the other hand, the average standard deviation for solids, TSS, TOC, and other components is larger than for all the ions (ca. 51%), which is a result of rapid changes of these components that can occur within one week of the oil sands mining operation. These rapid changes may have a significant impact on membrane performance since it could accelerate fouling and quickly reduce membrane specific flux.

A qualitative difference between all TNU streams (feed, retentate, and permeate) for a given set of conditions (50% stage cut, TMP: 5.3 bar) is shown in Fig. 8. Two permeate samples that come from two of the modules in series are also shown. The picture shows a dramatic difference between the recycle process water fed to the TNU and the produced permeate streams.

#### 4.1. Mass rejection of ions, TOC and TSS

Mass rejection, calculated using Eq. (4), as a function of TMP for two cations (Na<sup>+</sup>, Ca<sup>2+</sup>), two anions (HCO<sub>3</sub><sup>-</sup>, SO<sub>4</sub><sup>2-</sup>), as well as TOC and TSS are shown in Fig. 9a and b. These ions and components were selected as an example of the effect of ionic size and charge on rejection since they are found in large amounts in the recycle feed water and have different charge (positive or negative) and valence (+/- 1 and +/-2). It is important to highlight that although calcium is not among the ions

**Table 4**  
Recycle Process Water Components (Feed to TNU).

Ion/Compound	Range (mg/kg)	Mean (mg/kg)	Standard deviation (mg/kg)
<i>Cations</i>			
Lithium, Li <sup>+</sup>	0.1–0.2	0.1	0.0
Sodium, Na <sup>+</sup>	220.0–360.0	295.8	32.4
Potassium, K <sup>+</sup>	11.8–18.6	14.8	2.0
Magnesium, Mg <sup>2+</sup>	12.3–16.0	14.1	1.0
Calcium, Ca <sup>2+</sup>	25.1–34.1	29.3	2.6
Barium, Ba <sup>2+</sup>	0.1–0.2	0.2	0.0
Iron, Fe <sup>2+,3+</sup>	<0.02	–	–
Manganese, Mn <sup>2+</sup>	<0.005–0.1	–	–
Copper, Cu <sup>2+</sup>	<0.01	–	–
Phosphorus, P <sup>3+</sup>	<0.08	–	–
Aluminum, Al <sup>3+</sup>	<0.1–3.3	1.7	1.4
<i>Anions</i>			
Fluorine, F <sup>-</sup>	1.3–3.3	2.6	17.5
Bicarbonate, HCO <sub>3</sub> <sup>-</sup>	349.0–509.0	439.0	0.1
Chlorine, Cl <sup>-</sup>	103.0–167.0	136.9	1.4
Bromine, Br <sup>-</sup>	0.2–0.4	0.3	0.5
Nitrite, NO <sub>2</sub> <sup>-</sup>	<0.05–1.1	–	25.7
Sulphate, SO <sub>4</sub> <sup>2-</sup>	163.0–268.0	215.3	11.6
Nitrate, NO <sub>3</sub> <sup>-</sup>	0.1–2.7	0.9	0.3
Phosphate, PO <sub>4</sub> <sup>3-</sup>	< 0.2	–	0.5
<i>Compounds</i>			
Solids	39.2–4,452.3	865.0	1,122.4
TOC	31.0–134.0	47.2	19.1
TSS	13.0–305.0	139.8	75.6
Hardness (as CaCO <sub>3</sub> )	72.0–151.0	129.1	15.1
Silica (SiO <sub>2</sub> )	2.7–20.5	7.1	3.2
Total Silicon, Si	2.7–9.6	3.4	32.4
Total Boron, B	1.3–2.4	1.9	0.3
Total Sulphur, S	61.0–109.0	76.2	30.4

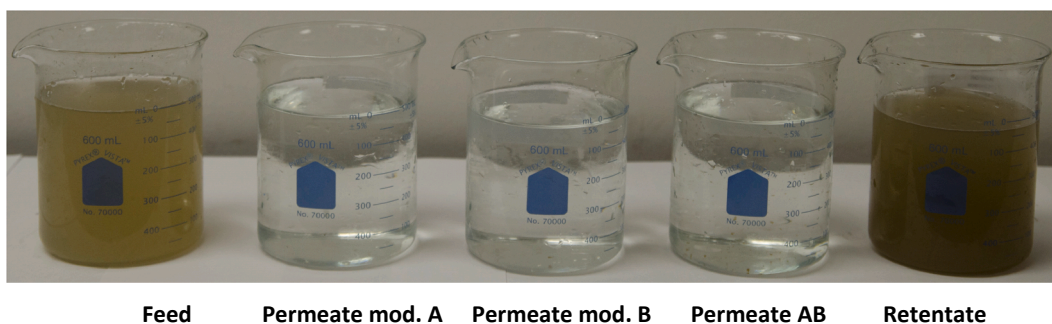


Fig. 8. TNU Samples at 50% stage cut and TMP: 5.3 bar.

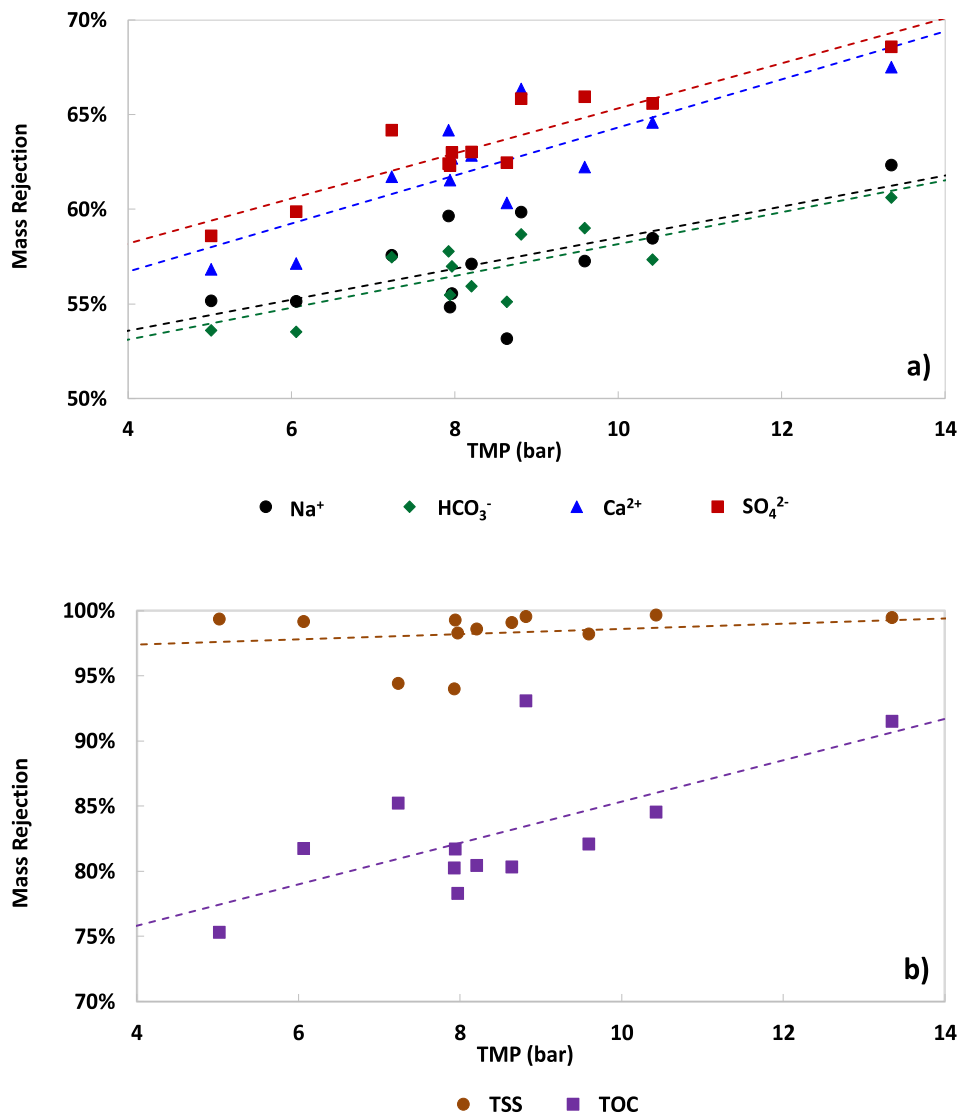


Fig. 9. a) Mass rejection of sodium, bicarbonate, calcium, and sulfate ions. b) Mass rejection of TOC and TSS. Both plots show data as a function of TMP at a Stage Cut of 50%. Lines must be regarded as a “guide for the eye”.

found in large quantities, it is one of the most important ions in this mine since high concentrations of calcium reduce oil recovery; therefore, regular monitoring of this ion is required in the oil extraction process. Other oil sands mines, depending on the mining area, could encounter oil recovery issues with other ions such as sodium or bicarbonate [35].

The data shown in Fig. 9 correspond to results collected in between cleanings in place (CIP). From this figure it is seen that the higher the

TMP, the higher the mass rejection. The relationship between mass rejection and TMP was found to be relatively linear at least within the TMP range measured. The lines displayed in Fig. 9 does not represent a physical model and are shown only to highlight the trends. These lines were calculated using a least-squares regression. It is important to note that the data in Fig. 9 show some scattering which is mainly attributed to fluctuations in the independent variables of the recycle process water,

analytical error, or sample contamination.

Based on the components of the recycle feed water, it is expected that TNU membranes could experience three types of fouling over time: inorganic, colloidal, and/or organic [22,24,36]. Inorganic fouling or scaling is caused by the accumulation of inorganic precipitates like silica and calcium carbonate (inorganic salts) on the membrane surface or within the pores. Other foulants can be suspended solids, silts, and clay which can create colloidal structures that could plug pores. Organic fouling might also occur due to the presence of bitumen in the recycle feed water. Considering the composition of recycle process water, colloidal fouling from inert particles such as silts and clays is expected to be predominant on the TNU membranes, although some inorganic and organic fouling are at play as well.

A way to visualize the effect of fouling is through reduction of membrane specific flux over time as it is displayed in Fig. S1. For this cycle, the specific flux was reduced by 63% over approximately 1,500 running hours. To remediate this type of fouling, a chemical cleaning in place (CIP) was performed in the TNU after approximately two months (1500 h) of continuous operation at 50% stage cut resulting in recovering the specific flux within 10% of pre-fouling values. In addition, high velocities in the re-circulation loop were maintained to reduce fouling in the system. The flow regime in the re-circulation loop was found to be turbulent ( $145,000 > Re < 296,000$ ) in the range of temperature of the

recycle feed water temperature (6–36 °C).

It is important to note that mass rejection of ions and components is restored after a cleaning in place (CIP) is performed as shown in Fig. S1. It is also considered that both TSS and TOC deposits on the membrane could be a major contributor to fouling and hence impact the ion rejection performance of the membrane. Fig. S2 shows that there is a positive correlation between ion rejection and TOC and TSS rejection. The correlation of ion rejection with TSS is not as clear as that of TOC since the values of TSS range very close to 100% rejection. Detailed characterization of the foulant components and a discussion on its influence on ions rejection will be given in a subsequent manuscript.

When analyzing the effect of the specific flux reduction over mass rejection of ions and components, it is observed in Fig. 10 that the lower the specific flux, meaning the more resistance to flow, the higher the mass rejection of ions and components. This behavior indicates a potential formation of a cake layer or solute-solute attachment on the membrane surface that is favouring the rejection of ions and solutes. A cake layer is formed when fouling layers are built up on each other [24]. The formation of a cake layer (surface layer), pore blocking, and pore adsorption are mechanisms that can contribute to irreversible fouling [36].

To better see potential trends resulting from differences in electrical charges and valences, the mass rejections vs. specific flux of all cations

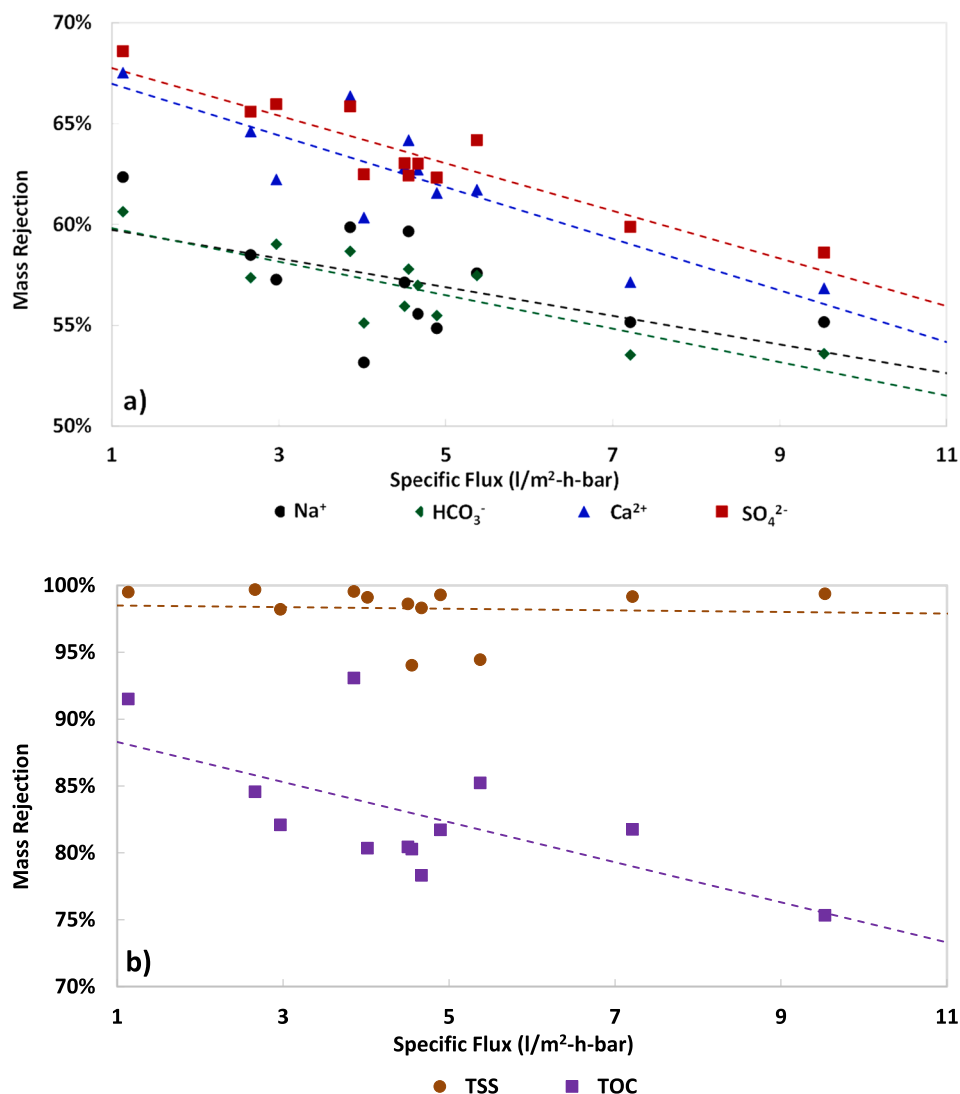


**Fig. 10.** a) Mass rejection of sodium, bicarbonate, calcium, and sulfate ions. b) Mass rejection of TOC and TSS. Both plots show data as a function of specific flux at a stage cut of 50%. Lines must be regarded as a “guide for the eye”.

and anions are displayed in Fig. S2. The lines in these figures were also found through least-square regression of the experimental data and must be regarded as a “guide for the eye”. The trends observed in Fig. S2a indicate that divalent cations ( $\text{Ba}^{2+}$ ,  $\text{Ca}^{2+}$ ,  $\text{Mg}^{2+}$ ) are preferentially rejected in comparison to monovalent ( $\text{K}^+$ ,  $\text{Na}^+$ ,  $\text{Li}^+$ ). In the case of anions (Fig. S2b), sulfate ( $\text{SO}_4^{2-}$ ) as divalent anion shows larger mass rejections than monovalent anions ( $\text{Br}^-$ ,  $\text{NO}_3^-$ ,  $\text{HCO}_3^-$ ,  $\text{F}^-$ ,  $\text{Cl}^-$ ). Bromine ( $\text{Br}^-$ ) presents a wider mass rejection range (20–67%) in comparison to the other monovalent ions. This could be the result of either an analytical error or the presence of another rejection mechanism. A few other outlier measurements could be distinguished in the plots; for instance, chloride mass rejection at a specific flux of  $1 \text{ l/m}^2\text{-h-bar}$  (42%, Fig. S2b) seems to be outside of the general trend based on the results obtained at a lower TMP.

The highest experimental mass rejection for all cations, anions, and components consistently occurred at the condition with the lowest specific flux value ( $1.13 \text{ l/m}^2\text{-h-bar}$ ). These experimental mass rejection values are listed in Table 5. Note that calcium had the second largest rejection (68%), an encouraging result considering the importance of this ion in the oil extraction process in this mine. For comparison purposes, this table also includes effective diameter values of non-hydrated and hydrated ions, organized from small to large hydrated diameter, as well as electrical charge and valence. The hydration of an ion depends on the electrostatic attraction of water molecules to that ion. This attraction depends on the ion's density of charge. Therefore, smaller ions attract more water molecules, resulting in an inverse relationship between non-hydrated and hydrated diameters [37].

As can be seen, the largest mass rejection of all the components given in Table 5 was for TOC and TSS. The high rejection seen for TOC (92%) is

**Table 5**  
Highest Experimental Mass Rejection (Constant stage cut: 50%).

Ion/Compound	Mass Rejection (%)	Hydrated ion diameter (nm) [38]	Non-hydrated ion diameter (nm) [38]
<i>Cations</i>			
Potassium, $\text{K}^+$	63%	0.30	0.16
Sodium, $\text{Na}^+$	62%	0.45	0.10
Lithium, $\text{Li}^+$	60%	0.60	0.08
Barium, $\text{Ba}^{2+}$	73%	0.50	0.21
Calcium, $\text{Ca}^{2+}$	68%	0.60	0.14
Iron, $\text{Fe}^{2+}$	- *	0.60	0.10
Manganese, $\text{Mn}^{2+}$	- *	0.60	0.10
Copper, $\text{Cu}^{2+}$	- *	0.60	-
Magnesium, $\text{Mg}^{2+}$	65%	0.80	0.09
Aluminum, $\text{Al}^{3+}$	- *	0.90	0.08
Phosphorus, $\text{P}^{3+}$	- *	-	-
<i>Anions</i>			
Chlorine, $\text{Cl}^-$	42%	0.30	0.19
Nitrate, $\text{NO}_3^-$	63%	0.30	-
Nitrite, $\text{NO}_2^-$	- *	0.30	-
Bromine, $\text{Br}^-$	67%	0.30	0.20
Fluorine, $\text{F}^-$	54%	0.35	0.15
Bicarbonate, $\text{HCO}_3^-$	61%	-	-
Sulphate, $\text{SO}_4^{2-}$	69%	0.40	-
Phosphate, $\text{PO}_4^{3-}$	- *	0.40	-
<i>Components</i>			
TOC	92%	**	**
TSS	100%	**	**
Hardness (as $\text{CaCO}_3$ )	66%	**	**
Silica ( $\text{SiO}_2$ )	58%	**	**
Total Silicon, Si	58%	**	**
Total Boron, B	58%	**	**
Total Sulphur, S	70%	**	**

\* Trace quantities in recycle process water Components (Feed to TNU).

- Data not available in same reference.

\*\* Non ions.

very encouraging for water usage in the oil sands process. The TOC components are mainly coming from the residual bitumen which, if unfiltered, can cause environmental issues and fouling in the process. The TSS had a rejection of 100%, which was expected considering that the pore size of the membranes is 0.9 nm. The high mass rejections of TOC and TSS are most likely due to sieving, since it is expected that these components have, on average, sizes larger than several nanometers. Other components such as calcium carbonate, silica, total silicon, total boron, and total sulphur showed a maximum mass rejections of 66%, 58%, and 70%, respectively.

In addition to a sieving effect, it is expected that electrostatic forces also act as a rejection mechanism for the ions due to differences in valences between cations and anions. To better illustrate the effect of valence and hydrated ion diameter on mass rejection, the experimental mass rejection (at  $1.13 \text{ l/m}^2\text{-h-bar}$ ) are depicted in Fig. 11 as a function of hydrated ion diameters. As can be seen from this figure, for cations with valence of +1 and +2, there is a clear decrease in mass rejection with an increment of ion diameter, and valences of +2 exhibit higher rejection values than +1.

When analyzing only the cations with a valence of +2 (Mg, Ca, and Ba), it can be noticed that magnesium has a hydrated diameter of 0.8 nm which is very close to the membrane pore size of 0.9 nm. This similarity in sizes could lead to the assumption that magnesium would be the most rejected cation if sieving effect was the most dominant rejection mechanism. However, that was not the case. Magnesium showed a rejection of 65%, which was lower in comparison to barium (73%) that has a hydrated diameter of 0.5 nm. Similar trends are observed for the cations with a valence of +1. These differences indicate that not only a sieving effect but also in parallel an electrostatic phenomenon influences the cations mass rejection.

Doing the same analysis among the anions with a valence of -1, bromine presented the largest mass rejection (67%) and fluorine the lowest (54%), although bromine has a smaller hydrated ion size (0.30 nm) than fluorine (0.35 nm). Sulfate, the only anion with a valence of -2 in the Fig. 11 and with a hydrated-ion size of 0.4 nm, showed the largest maximum rejection (69%) among all the anions. Hence, a similar sieving and electrostatic effects are also observed for the anions. Note that chlorine had a rejection of 42% but this value seems to be an outlier based on the trends obtained in the studied range of specific flux (see Fig. S2).

One way to look at the effect of an electrostatic phenomenon is through charge density as a measure to determine the strength at which cations and anions are attracted or rejected by the membrane. In this study, charge density is defined as the ratio of valence and the hydrated ion radii. It is considered that the hydrated ions should have the same electrical charge as the non-hydrated ions by conservation of charge. The effect of charge density on mass rejection for both cations and anions is illustrated in Fig. 12a and b respectively, where it is observed that the higher the ion charge density, the larger the mass rejection.

For cations, there is a clear trend of higher charge densities yielding higher rejections. Monovalent and divalent cations both follow the same trend when using charge density values since its valence is included as part of the calculation. Note that for cations with the same hydrated ion size, as in the case of calcium and lithium (0.6 nm), a higher electrical charge enhances the ion rejection. These observations could be originally attributed to an adsorption effect considering that the membrane is negatively charged, as discussed before in Section 2.2. Furthermore, it could be assumed that the fouling layer also exhibits an electrical charge, which enhances ions rejection.

Similarly, anions rejection is larger with an increment in charge density. However, a different phenomenon occurs here, and this increase in rejection could be attributed to repulsion forces from the negative surface of the membrane or the fouling layer instead. If only electrostatic repulsion is considered, the anions would be dominant in the retentate, resulting in an imbalance of charge at both sides of the membrane. Hence, as the anions are rejected then the cations must be

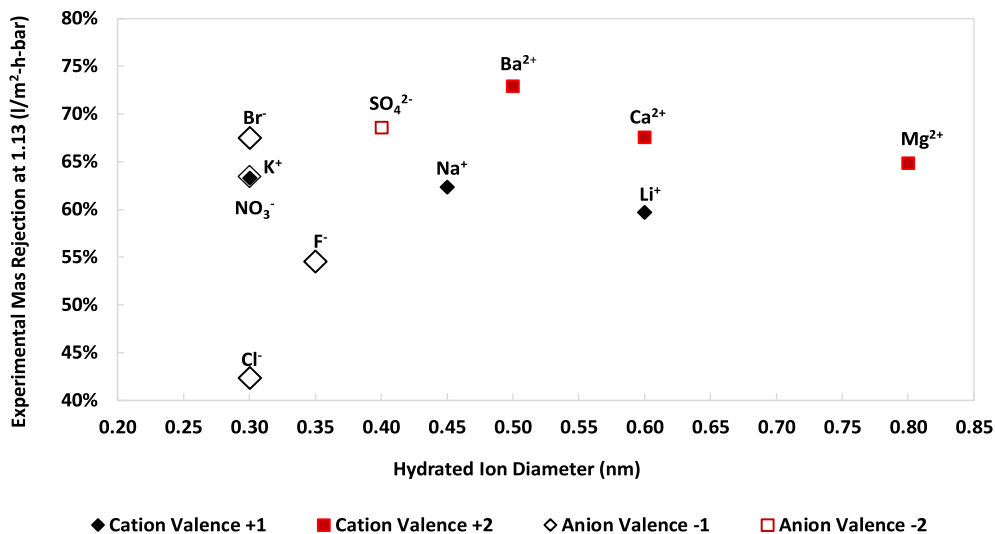


Fig. 11. Experimental mass rejection at 13.3 bar vs. Hydrated Ion diameter.

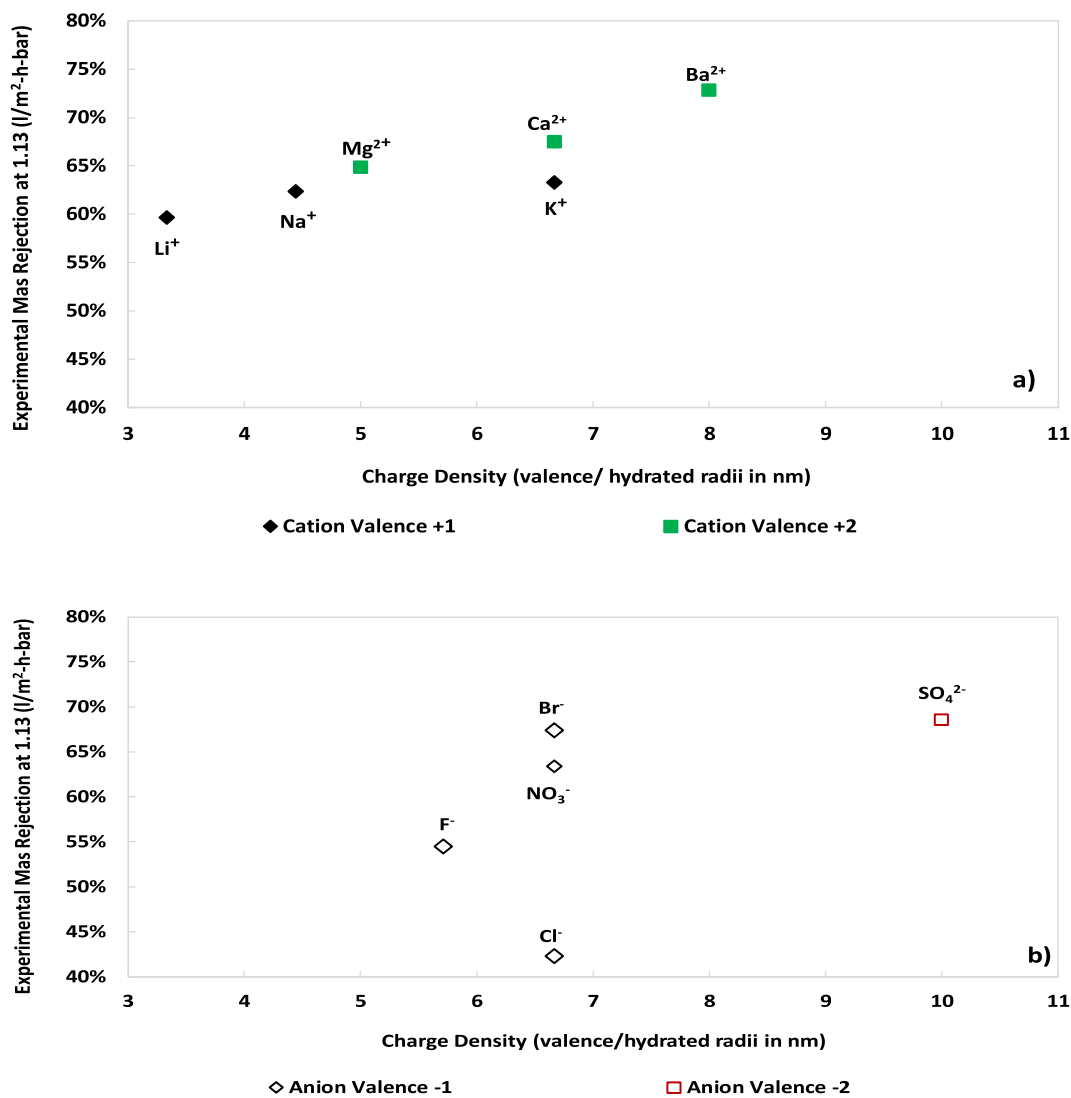


Fig. 12. Experimental mass rejection at 13.3 bar vs. Charge Density a) Cations b) Anions.

rejected to counteract the potential difference across the membrane in order to maintain electroneutrality [29].

## 5. Conclusions

The first of its kind commercial pilot unit with titania ceramic nanofiltration membranes (TNU) has been tested for almost two years in a Canadian oil sands mine under actual oil sands recycle process water characteristics. No chemical or physical pre-treatment of the recycle process water was used during any of the tests. The tests evaluated in this work were done at a 50% stage cut or permeate yield. A dramatic difference in clarity was observed between the recycle process water fed to the TNU and the produced permeate streams. Results also showed a reduction of specific flux over time which can be interpreted as fouling. A potential formation of a cake layer or solute–solute attachment on the membrane surface seems to favour the rejection of ions and solutes. Results show that the lower the specific flux, the higher the mass rejection of ions and components.

Total Suspended Solids (TSS) were rejected almost 100% and Total Organic Carbon (TOC) rejection was above 75% at all conditions. The high mass rejections of TOC and TSS are most likely due to sieving, since it is expected that these components have, on average, sizes larger than the membrane pore size (>0.9 nm). This is a very encouraging result in terms of water usage in the oil sands mining process since most of the organic components are coming from residual bitumen (high molar mass viscous petroleum fluid).

The titania membrane showed a preference for rejecting ions with high charge density, both cations and anions. Since the membrane is negatively charged, based on pH and IEP, it is possible to infer that cations are rejected at high density charges due to adsorption to the membrane. For anions, it is observed that the higher the charge density, the higher the rejection. This might be explained by electrical repulsion since the membrane has the same charge. The distribution of cations and anions is expected to maintain electroneutrality in the system. Results indicated that both ionic size differences and electrostatic interactions influenced the rejection of ions and components.

Overall, it was found that it is possible to implement ceramic nanofiltration membranes in the oil sands mines and obtain significant water quality improvements. It is considered that the permeate stream from the ceramic nanofiltration unit could be used as a feed to the existing conventional reverse osmosis system in the oil sands mine for further polishing. This will reduce the river water intake, meaning that oil sands operators would be storing less process water in the tailings ponds.

## Declaration of Competing Interest

The authors declare that they have no known competing financial interests or personal relationships that could have appeared to influence the work reported in this paper.

## Acknowledgements

The authors are grateful to Alberta Innovates Technology Futures (AITF) and Andreas Junghans GmbH & Co. KG. The authors also thank Dr. Jeffrey McCutcheon for his valuable feedback to the manuscript. Finally, special thanks to a very supportive Operations and Process Innovation Teams that made possible to run the TNU during all Canadian seasons.

## Appendix A. Supplementary data

Supplementary data to this article can be found online at <https://doi.org/10.1016/j.seppur.2020.117821>.

## References

- [1] Alberta Government, Alberta Oil Sands Industry: Quarterly Update Summer 2018, (2018) 18. [www.albertacanada.com](http://www.albertacanada.com).
- [2] R.J. Chalaturnyk, J.D. Scott, B. Özüm, Management of oil sands tailings, *Pet. Sci. Technol.* 20 (2002) 1025–1046, <https://doi.org/10.1081/LFT-120003695>.
- [3] M.A. Carrigy, Guide To The Athabasca Oil Sands Area, *Can. Soc. Pet. Geol. Oil Sands Symp.* (1974) 213. [http://www.ags.gov.ab.ca/publications/inf/pdf/inf\\_065.pdf](http://www.ags.gov.ab.ca/publications/inf/pdf/inf_065.pdf).
- [4] Oil Sands Magazine, Water Usage, (2018). <http://www.oilsandsmagazine.com/technical/environment/water-usage> (accessed July 21, 2018).
- [5] Alberta Energy Regulator, Alberta Energy Industry Water Use Report, 2016. [www2.aer.ca](http://www2.aer.ca).
- [6] Canada's Oil and Natural Gas Producers (CAPP), Canada's Oil Sands, 2018. [www.canadaoilsands.ca](http://www.canadaoilsands.ca).
- [7] J.P. Giesy, J.C. Anderson, S.B. Wiseman, Alberta oil sands development, *Proc. Natl. Acad. Sci.* 107 (2010) 951–952, <https://doi.org/10.1073/pnas.0912880107>.
- [8] C. Energy, Oil sands, Water Manage. (2016) 2014–2015. <http://www.cenovus.com/operations/oilsands.html>.
- [9] E.W. Allen, Process water treatment in Canada's oil sands industry: I. Target pollutants and treatment objectives, *J. Environ. Eng. Sci.* 7 (2008) 123–138, <https://doi.org/10.1139/s07-038>.
- [10] A.W.W. Association, Water Treatment: Membrane Processes, 1st ed., McGraw-Hill Professional, New York, 1996.
- [11] M. Hemati, M.R. Sebzari, F. Rekabdar, T. Mohammadi, S.R.H. Abadi, Ceramic membrane performance in microfiltration of oily wastewater, *Desalination*. 265 (2010) 222–228, <https://doi.org/10.1016/j.desal.2010.07.055>.
- [12] H.M. Deriszadeh Ali, H. Thomas, Produced Water Treatment by Micellar-Enhanced Ultrafiltration, *Environ. Sci. Technol.* 44 (2010) 1767–1772.
- [13] H. Peng, K. Volchek, M. MacKinnon, W.P. Wong, C.E. Brown, Application on to nanofiltration to water management options for oil sands operation, *Desalination*. 170 (2004) 137–150, <https://doi.org/10.1016/j.desal.2004.03.018>.
- [14] E.S. Kim, Y. Liu, M.G. El-Din, The effects of pretreatment on nanofiltration and reverse osmosis membrane filtration for desalination of oil sands process-affected water, *Sep. Purif. Technol.* 81 (2011) 418–428, <https://doi.org/10.1016/j.seppur.2011.08.016>.
- [15] M.A. Farrukh, Nanofiltration, *IntechOpen* (2018), <https://doi.org/10.5772/intechopen.70909>.
- [16] K. Loganathan, P. Chelme-Ayala, M. Gamal El-Din, Effects of different pretreatments on the performance of ceramic ultrafiltration membrane during the treatment of oil sands tailings pond recycle water: A pilot-scale study, *J. Environ. Manage.* 151 (2015) 540–549, <https://doi.org/10.1016/j.jenvman.2015.01.014>.
- [17] A. Lobo, Á. Cambiella, J.M. Benito, C. Pazos, J. Coca, Ultrafiltration of oil-in-water emulsions with ceramic membranes: Influence of pH and crossflow velocity, *J. Memb. Sci.* 278 (2006) 328–334, <https://doi.org/10.1016/j.memsci.2005.11.016>.
- [18] Z. Sadeghian, F. Zamani, S.N. Ashrafizadeh, Removal of oily hydrocarbon contaminants from wastewater by  $\gamma$ -alumina nanofiltration membranes, *Desalination*. 20 (2010) 80–85, <https://doi.org/10.5004/dwt.2010.1154>.
- [19] R.M.H. Amin Sh.K., Abdallah H.A.M., An Overview of Production and Development of Ceramic Membranes, *Int. J. Appl. Eng. Res.* 11 (2016) 7708–7721.
- [20] V.V. Tarabara, L.M. Corneal, S. Byun, A.L. Alpatova, S.J. Masten, S.H. Davies, M. J. Baumann, Mn oxide coated catalytic membranes for a hybrid ozonation–membrane filtration: Comparison of Ti, Fe and Mn oxide coated membranes for water quality, *Water Res.* 45 (2010) 163–170, <https://doi.org/10.1016/j.watres.2010.08.031>.
- [21] M. Mueller, Uwe Witte, Ceramic membrane applications for spent filter backwash water treatment, 2008. [www.TZW.de](http://www.TZW.de).
- [22] A. Duraisamy, R. T., Beni, A. H., and Henni, State of the Art Treatment of Produced Water, in: 2013: pp. 199–222. <http://doi.org/10.5772/53478>.
- [23] S.M. Samaei, S. Gato-Trinidad, A. Altaee, The application of pressure-driven ceramic membrane technology for the treatment of industrial wastewaters – A review, *Sep. Purif. Technol.* 200 (2018) 198–220, <https://doi.org/10.1016/j.seppur.2018.02.041>.
- [24] V. Gitis, G. Rothenberg, Ceramic membranes : new opportunities and practical applications, Wiley-VCH, Weinheim, 2016.
- [25] P. Puhlfürb, A. Voigt, R. Weber, M. Morbé, Microporous TiO<sub>2</sub> membranes with a cut off < 500 Da, *J. Memb. Sci.* 174 (2000) 123–133.
- [26] I. Voigt, H. Richter, M. Stahn, M. Weyd, P. Puhlfürb, V. Prehn, C. Günther, Scale-up of ceramic nanofiltration membranes to meet large scale applications, *Sep. Purif. Technol.* (2019) 329–334, <https://doi.org/10.1016/j.seppur.2019.01.023>.
- [27] M. Weyd, H. Richter, I. Voigt, Membrane activities at Fraunhofer IKTS Membrane activities at Fraunhofer IKTS, (n.d.).
- [28] V.M. Gun'ko, V.I. Zarko, V. V. Turov, R. Leboda, E. Chibowski, E.M. Pakhlov, E. V. Goncharuk, M. Marciniak, E.F. Voronin, A.A. Chuiko, Characterization of fumed alumina/silica/titania in the gas phase and in aqueous suspension, *J. Colloid Interface Sci.* 220 (1999) 302–323. <http://doi.org/10.1006/jcis.1999.6481>.
- [29] F. Liang, Ceramic nanofiltration membrane for ions separation from ion exchange brine: effect of ionic strength and salts on ionic rejection, *Delft University of Technology*, 2018.
- [30] H. Tamura, K. Mita, A. Tanaka, M. Ito, Mechanism of Hydroxylation of Metal Oxide Surfaces, *J. Colloid Interface Sci.* 243 (2001) 202–207, <https://doi.org/10.1006/JCIS.2001.7864>.
- [31] E.W.J. Mardles, Viscosity of Suspensions and the Einstein Equation, *Nature*. 145 (1940) 970, <https://doi.org/10.1038/145970a0>.

- [32] ACOSA, Determination of the Bitumen, Water and Solids in Oil Sand - Dean Stark Method, (1984) 1–18.
- [33] E.E.W. Rice, R.B. Baird, A.D. Eaton, in: A.D. Eaton, E.W. Rice, R.B. Baird (Eds.), *Standard Methods for the Examination of Water and Wastewater; Procedures 2540D, 2540C and 5310B*, 23rd ed., American Public Health Association, American Water Works Association, Water Environment Federation, Washington, D.C, 2017.
- [34] C.S. Griffith, G.D. Sizgek, E. Sizgek, N. Scales, P.J. Yee, V. Luca, Mesoporous Zirconium Titanium Oxides. Part 1: Porosity Modulation and Adsorption Properties of Xerogels, *Langmuir* 24 (2008) 12312–12322, <https://doi.org/10.1021/la801464s>.
- [35] J.H. Masliyah, J. Czarnecki, Z. Xu, *Handbook on theory and practice of bitumen recovery from Athabasca oil sands - Volume 1: Theoretical basis*, Kingsley Knowl Publ. (2011) 115–116.
- [36] N.L. Le, S.P. Nunes, Materials and membrane technologies for water and energy sustainability, *Sustain. Mater. Technol.* 7 (2016) 1–28, <https://doi.org/10.1016/j.susmat.2016.02.001>.
- [37] B.E. Conway, *Ionic Hydration In Chemistry and Biophysics*, Elsevier Scientific Publishing Company, 1981.
- [38] J. Kielland, Individual Activity Coefficients of Ions in Aqueous Solutions, *J. Am. Chem. Soc.* 59 (1937) 1675–1678, <https://doi.org/10.1021/ja01288a032>.